REPORT DOCUMENTATION PAGE

Form Approved
OMB No. 0704-0188

1. AGENCY USE ONLY (Leave blank)	2. REPORT DATE	3. REPORT TYPE AND DATES COVERED
	10/16/97	Technical Report, May 96 - Sept. 97

4. TITLE AND SUBTITLE
Formation of Thin-Films of CdTe, CdSe, and CdS by Electrochemical ALE

5. FUNDING NUMBERS
G-N00014-19-J-1919
96 Pro - 2855
R&T 4133036

6. AUTHOR(S)
Lisa P. Colletti, Billy H. Flowers, Jr. and John L. Stickney

7. PERFORMING ORGANIZATION NAME(S) AND ADDRESS(ES)
Department of Chemistry
University of Georgia
Athens, GA 30602-2556

8. PERFORMING ORGANIZATION REPORT NUMBER
Technical Report #27

9. SPONSORING / MONITORING AGENCY NAME(S) AND ADDRESS(ES)
Office of Naval Research
Chemistry Division
800 North Qunicy Street
Arlington, VA 22217-5660

10. SPONSORING / MONITORING AGENCY REPORT NUMBER

11. SUPPLEMENTARY NOTES

12a. DISTRIBUTION / AVAILABILITY STATEMENT
Approved for public release and sale: its distribution is unlimited

12b. DISTRIBUTION CODE

13. ABSTRACT *(Maximum 200 words)*

Thin-films of CdTe, CdSe, and CdS have been electrodeposited by electrochemical atomic layer epitaxy (ECALE), using an automated electrochemical deposition system. Previous reports of an automated system for forming ECALE deposits involved use of a small thin layer flow cell, which evidenced several drawbacks. Conversion of the thin layer cell to a thick layer design resulted in greatly improved deposit quality and reproducibility. Deposits were analyzed using electron probe microanalysis (EPMA), scanning electron microscopy (SEM), and grazing-incident X-ray diffraction (XRD). The results were consistent with a layer by layer growth mode, and the principles of atomic layer epitaxy. CdTe films were grown using up to 1000 ECALE cycles, and were stoichiometric through 500. The 1000 cycle films were a few percent rich in Te, under the conditions used. CdSe and CdS films formed also contained some excess chalcogenide, probably the result of less than ideal deposition parameters. Increasing amounts of particulates and surface roughening were observed for the 500 and 1000 cycle CdTe and CdSe films, relative to the 200 cycle deposits normally formed. This roughening may result from the excess chalcogenide. X-ray diffraction of the films indicated cubic crystal structures with preferred (111) orientations, for all three compounds.

14. SUBJECT TERMS	15. NUMBER OF PAGES
CdTe, CdSe, CdS, UPD, ECALE, ALE, electrodeposition	36
	16. PRICE CODE

17. SECURITY CLASSIFICATION OF REPORT	18. SECURITY CLASSIFICATION OF THIS PAGE	19. SECURITY CLASSIFICATION OF ABSTRACT	20. LIMITATION OF ABSTRACT
Unclassified	Unclassified	Unclassified	UL

Office of Naval Research
Grant N00014-91-J-1919
R&T Code 4133036
96PRO-2855

Technical Report No. 27

Formation of Thin-Films of CdTe, CdSe, and CdS by Electrochemical ALE

By Lisa P. Colletti, Billy H. Flower, Jr., and John L. Stickney

Prepared for Publication in the Journal of the Electrochemical Society

Department of Chemistry
University of Georgia
Athens, GA 30602-2556

October 15, 1997

Submitted to the *Journal of the Electrochemical Society*

Submitted JECS 7/23/97

Formation of Thin-Films of CdTe, CdSe, and CdS by Electrochemical ALE

Lisa P. Colletti, Billy H. Flower, Jr., and J.L. Stickney*
Chemistry Department, University of Georgia, Athens, Georgia 30602
Phone 706 542-1967
Fax 706 542-9454
Stickney@sunchem.chem.uga.edu

*To whom correspondence should be addressed

Abstract

Thin-films of CdTe, CdSe, and CdS have been electrodeposited by electrochemical atomic layer epitaxy (ECALE), using an automated electrochemical deposition system. Previous reports of an automated system for forming ECALE deposits involved use of a small thin layer flow cell, which evidenced several drawbacks. Conversion of the thin layer cell to a thick layer design resulted in greatly improved deposit quality and reproducibility. Deposits were analyzed using electron probe microanalysis (EPMA), scanning electron microscopy (SEM), and grazing-incident X-ray diffraction (XRD). The results were consistent with a layer by layer growth mode, and the principles of atomic layer epitaxy. CdTe films were grown using up to 1000 ECALE cycles, and were stoichiometric through 500. The 1000 cycle films were a few percent rich in Te, under the conditions used. CdSe and CdS films formed also contained some excess chalcogenide, probably the result of less then ideal deposition parameters. Increasing amounts of particulates and surface roughening were observed for the 500 and 1000 cycle CdTe and CdSe films, relative to the 200 cycle deposits normally formed. This roughening may result from the excess chalcogenide. X-ray diffraction of the films indicated cubic crystal structures with preferred (111) orientations, for all three compounds.

Introduction

The physical properties of cadmium chalcogenide semiconductors, are well suited for use as thin-film materials in the emerging opto-electronic industry [1, 2]. In many of the devices these thin-films play a part in, the fabrication procedures comprise a large percentage of the total cost [3], as the thin films have traditionally been deposited by expensive, high temperature, vacuum based techniques. An alternative method of fabrication, electrodeposition [4, 5, 6, Rajeshwar, 1992 #368, 7, 8], has attracted significant attention, due a number of possible advantages over vacuum based techniques, including: low temperature processing, uniform coverage of irregularly shaped features, and more facile waste handling [3, 9-11]. In addition, it has traditionally been an inexpensive and simple industrial technique, scalable to large dimensions [2, 3, 10, 12].

The most commonly used electrodeposition technique for the cadmium chalcogenides has been "codeposition" [4, 5, 6, Rajeshwar, 1992 #368, 7, 8], a method pioneered by Hodes et al. [13] and Kroger et al. [14]. Codeposition, however, has frequently resulted in deposits with poor crystallinity [15] and side products [16]. Since defects play a major role in limiting the efficiency of thin film devices [17], the growth of large grained stoichiometric films, with minimal grain boundaries [18], is desired.

Our group has been working on the electrochemical analog of atomic layer epitaxy (ALE) [19-22]. ALE is a method for forming thin films of materials an atomic layer at a time, using surface limited reactions. The electrochemical analog, electrochemical atomic layer epitaxy (ECALE) [7, 23], is being developed in an effort to improve control over electrodeposit morphology, stoichiometry and structure. Surface limited reactions are used in ALE to form each atomic layer, in order to prevent three dimensional growth and to promote epitaxy. In electrochemical ALE, surface limited reactions are used as well. Surface limited electrochemical reactions are well known, being referred to as underpotential deposition (UPD) [24, 25]. UPD occurs when it is more energetically favorable for one element to deposit on another element than for it to deposit on itself, due to the free energy of compound formation. Once the surface is coated with the first element, no more of the substrate element is available to react, and

deposition will stop. In an ECALE cycle, a second element would then be introduced and a second UPD reaction run, proceeding until the entire surface is coated. The net result of both reactions should be the formation of a monolayer of the compound. Films are formed by alternating the two UPD reactions in a cycle. The thickness is then determined by the number of cycle used.

Use of an ECALE cycle to form deposits provides a unique opportunity to decompose the deposition process into a series of individual steps, with each step becoming an adjustable parameter. Each step is then individually optimized, for instance each element is deposited from a separately optimized solution, at a separate potential. In this way, ECALE can act as a window into the mechanism of compound electrodeposition. Most other electrodeposition methodologies [4, 5, 6, Rajeshwar, 1992 #368, 7, 8] are limited in this respect, as the composition of a single solution and a single deposition potential are the only easily adjusted parameters.

Initially, ECALE deposits were formed using a thin layer electrochemical cell (TLEC), operated manually [7, 23], and each cycle would required about fifteen operations. Deposition of over 10 ECALE cycles proved very tedious. Automation of the deposition process was thus a necessity. The first automated systems were developed around a simple thin-layer flow cell design, very similar to commercial cells used in electrochemical HPLC detectors. Several benefits were felt to result from the thin layer cell, such as less solution, less waste, and less contamination. However, development of that system proved to be a slow series of small improvements and tedious problems with every component in the system [26]. The most problematic component proved to be the thin-layer electrochemical cell itself. Problems with uncompensated resistance (R_u), bubbles and edge effects, resulted in irreproducible results.

To minimize R_u, the cell shown in Figure 1A was built, in which a Vicor frit separated the reference and auxiliary electrodes from the thin layer cell volume. The frit was located directly over the center of the working electrode, flush with the interior face of the Plexiglas face plate (the R_u was on the order of 1-2 KΩ). In this configuration, however, the frit appeared to act as a

reservoir for Cd and Te species, possibly resulting in some cross contamination [26]. One design which avoids this problem is shown in Figure 1B, where the frit is in the out flow tube, so any particles resulting from cross contamination in the frit, will be flushed out and not have a chance of contaminating the substrate. Some increase in R_u did result from this configuration, however.

Solution flow through the cell was severely compromised by trapped bubbles and edge effects. It is not clear where the bubbles originated, its possible that some resulted from N_2 coming out of solution with pressure changes from the delivery tube to the cell. Bubbles could also result from loose fittings, or H_2 formation in the cell. Once formed, the bubbles were hard to dislodge, and interrupted solution flow and deposition. An example of the effects of trapped bubbles can be seen in Figure 2. Edge effects were also unpredictable, basically correlating with the roughness of the gasket edges, and the material it was made from.

The problems discussed above, combined to produce widely varying thin films from run to run, resulting in little progress in understanding the dependence of the deposit morphology, composition, and structure on steps in the ECALE cycle [26]. As most of these problems appear to be related to the use of a thin-layer electrochemical cell configuration, a standard H-cell was modified, Figure 3, to allow solutions to be pumped in and out. This design greatly reduced R_u, and eliminated solution flow problems due to bubbles and gasket edge effects. The H-cell configuration was not idea, but it did result in reproducible deposits, allowing studies of the formation of CdTe, CdSe, and CdS, presented here. Studies of the importance of a number of cycle variables on the deposition of CdTe will be published as well [27]

Experimental/Instrumentation

A schematic drawing of the deposition system used in the present studies is shown in Figure 4. It is similar to that previously used with the thin layer electrochemical cell configuration [26], but incorporating the modified H-cell shown in Figure 3. A standard H-cell was modified by attaching a rectangular compartment (5/8 in. x 1/4 in. x 1 in.) to the bottom, separated from the

auxiliary and reference electrode compartment by a fine glass frit (Figure 3). Using a frit within in the cell compartment was less than ideal, as some ions were trapped by the frit, possibly resulting in cross contamination [26]. At present, this does not appear to be a major problem, due to the vertical placement of the substrate, and the larger distance of the substrate from the frit, compared with the thin layer designs shown in Figure 1. A solution inlet/outlet port, Pyrex glass with a Teflon stopcock, was located at the bottom of the cell. It was fitted with 1/4-28 glass threads, allowing connection to standard low pressure LC fittings. A glass tube at the top of the H-cell, with a Teflon metering stopcock, allowed N_2 gas to flow continuously over the top of the solution during the deposition.

The increased volume of the H-cell (3 mL versus 10 μL for a thin layer cell) requires both larger solution reservoirs and higher solution flow rates. Four liter bottles were used for the Cd and Te containing solutions while the blank solutions were held in 19 L Pyrex bottles. Each 200 cycle experiment used slightly less than a liter of each electroactive solution, 3 L of the Cd blank , and 4.5 L of the Te or Se blank or 3L of the S blank. In this way, four 200 cycle experiments could be run before new solutions were needed.

The design of the system requires the use of one pump for each solution line. Small peristaltic pumps were used in this instrument (Figure 4), constructed with 3 roller pinchers and operated at 120 rpm. Tygon peristaltic tubing (2.79 mm ID) was used for the solutions, as it has reasonable levels of chemical resistance and low oxygen permeability. Average flow rates of approximately 56 ml/min were used. PEEK tubing, 1/8 in. OD, was used to connect the peristaltic tubing to the distribution valve, with PEEK 1/4-28 finger-tight fittings, again chemical resistance and low oxygen permeability were the primary reasons for choosing PEEK. A Masterflex Quick Load peristaltic pump head, coupled to a 200 RPM motor was used for rapid draining of the deposition cell.

Solution exchange was facilitated using a C25 Cheminert Valco six way selection valve (VICI) which was controlled by a Thar Design, Inc. Smart Valve Actuator. This valve has a minimal internal volume, which is completely flushed with the introduction of each new solution.

Previous work was side tracked because distribution valves used had unflushed internal volumes that promoted cross contamination [26].

Substrates were made from Si (100) wafers (International Wafer Service), coated (EMF Corporation) with approximately 5 nm of Ti or Cr followed by 200 nm of Au by vacuum evaporation. The sample substrates were cut to approximately 1/4 in. by 1 1/2 in. pieces, for each experiment, and mounted in a stainless steel holder, designed and constructed in house. The holders also provided electrical contact to the gold film. Once mounted each sample was rinsed twice in water, ethanol, and acetone. The last rinse of acetone was followed by a third rinse in water.

Solutions were prepared with 18 MΩ water from a Barnstead NANOpure water filtration system, fed with the departmental deionized water supply. Supporting electrolytes for the deposition of CdTe were 0.5 M Na_2SO_4, while 0.5 M $NaClO_4$ was used in the deposition of CdSe and CdS. Two solutions were used for each element, one containing the elemental precursor, and a corresponding "blank" solution, with no precursor present. The 0.5 mM $HTeO_2^+$ solution was made with TeO_2 (99.9995%, Puratronic) and 10 mM borate buffer, pH 9.2. Two $HSeO_3^-$ solutions were used. The first 5.0 mM $HSeO_3^-$ solution was made with SeO_2 (99.9995%, Aldrich) and a 5 mM acetic acid buffer, pH 4.5, while in a second solution, the acetic acid buffer was replaced with a 10 mM sodium borate buffer, pH 9.2. The S^{2-} solutions were made daily (to prevent decomposition) with 1 mM $Na_2S \bullet 9H_2O$ (99.9%, Fisher Scientific) and resulted in a pH of 10.5. The S blank solution was adjusted to pH 10.5 by the addition of NaOH. The Cd^{2+} solutions were made with 5.0 mM $CdSO_4$ (99.9995%, Aldrich) and 50 mM acetate, adjusted to pH 5.7.

A Jena Jenavert optical microscope was used for visible inspection of the deposits. Scanning electron micrographs were taken on either a Philips 505 equipped with an energy dispersive X-ray detectors or a Hattachie field emission scanning electron microscope (FESEM). Electron probe microanalysis (EPMA) was performed on a JEOL JXA-8600 superprobe, equipped with four-wave length dispersive X-ray spectrometers and an energy dispersive

detector. A Sintag 2000 diffractometer equipped with a liquid nitrogen-cooled, intrinsic, germanium solid state detector and a normal-focus copper X-ray tube powered at 40 mA, 40 KeV was used for X-ray diffraction (XRD) studies. Grazing angle scans were done using a thin film attachment.

Results and Discussion

The UPD of Cd, Te, Se, and S have been previously examined in this group, using thin layer electrochemical cells [23, 28, 29]. The UPD of Cd take place reductively from $CdSO_4$, to the extent of about 0.3 – 0.5 ML (monolayers) [30-33]. In addition, at potentials near the onset of bulk Cd deposition, current associated with the formation of a Au-Cd alloy is observed [30]. UPD of sulfur from sulfide solutions occurs oxidatively [28, 34, 35]. The UPDs of Se and Te are complicated by the fact that, unlike S^{2-}, Se^{2-} and Te^{2-} are not very stable in aqueous solutions. They tend to react with even traces of O_2, to form the corresponding element. Atomic layers of Se and Te can still be formed using solutions of $HSeO_3^-$ and $HTeO_2^-$, respectively, which are stable. However, since the potentials needed for reductive UPD of Se and Te from these solutions are sufficiently positive that the Cd is no longer stable, a two step deposition process was developed. The first step involved the deposition of a monolayer or two of the bulk element from the $HSeO_3^-$ or $HTeO_2^+$ solution. The second step was to reductively strip the bulk element, forming Se^{2-} or Te^{2-}, and leaving an atomic layer of Te or Se on the surface. The second (stripping) step was performed in a blank solution, containing no $HSeO_3^-$ or $HTeO_2^+$ [26].

ECALE cycles were developed using the reactions mentioned above. Refinements were conducted by forming thin-films, 1-10 cycles, using a manual thin layer cell [23, 28, 29]. Those

results were then used as a starting point in programming the initial ECALE cycles in the automated systems [26].

Figure 5 is a diagram of an ECALE cycle, developed for automated deposition of CdTe [7, 26]. Valve and pump operations are coupled and represented in the upper part of the figure. Small squares represent single rinses of solution, into and out of the cell. Squares with a dashed sideline indicate that the solution was not immediately drained from the cell but was held there for the time stipulated under "Quiescent", corresponding to the deposition and stripping times. The lower part of the figure displays the potentials applied to the substrate during the cycle. CdTe ECALE cycles used -0.6 V for Cd UPD, -0.8 V for bulk Te deposition, and -1.25 V for Te stripping.

CdTe Thin-Films

The first test of the new hardware setup was to form a series of CdTe deposits formed using 50 to 1000 CdTe ECALE cycles. The resulting CdTe thin film deposits showed an impressive array of interference colors as a function of thickness. The deposits appeared brown after 50, pink after 100, purple after 150, royal blue after 200, gold green after 500, and an opaque, pinkish gold after 1000 cycles.

Using FESEM the morphology of the substrate surface, prior to deposition, can be examined (Figure 6A). The surface appears to be coated with small nodules, even though the substrates are optically flat mirrors to the eye, they are quite rough at the 300 nm scale of Figure 6A. Scanning tunneling microscopy has shown these nodules to be composed of small terraces or steps approximately 10 nm in width, well ordered and (111) oriented. Figure 6B shows the

substrate after 200 cycles of CdTe deposition. The similarity of the substrate and deposit is encouraging, as it is consistent with a layer-by-layer growth mode.

SEM micrographs of films up to 200 ECALE cycles, Figure 7A, appear very smooth, with little or no three dimensional growth evident. The particles in the micrograph were used for focusing, as the films were otherwise featureless. All of the films made with 50 to 200 cycles contained some type of widely scattered particles (diameter>1μm) usually found more than 50 μm apart. The origin of these particles is not clear, they may just be small pieces of dust. Other sources of particles include cross contamination, mixing of solutions in the H-cell's frit, poor deposition conditions, or micro-dendritic tellurium growth. EPMA of some particles show large excesses of Te, which supports the idea of micro-dendritic tellurium. Maurin and Pottier [36] saw examples of dendritic behavior, although on the scale of 5-10 μm, during codeposition of CdTe. They suggest that nucleation of this type of defect is likely to occur at cracks in the film.

Scanning electron microscopy of 500 ECALE cycles (Figure 7B) shows a surface with a large number of small particulates scattered across the surface. These features increase in size and density as the number of cycles increases, demonstrated by the 1000 cycle deposit (Figure 7C). Presently, it is believed that this morphology results from non-idealities in the two step Te atomic layer deposition process, described above, that results in Te features. Several layers of Te are first put down, and then the excess is removed. It is possible that under some conditions, not all of the excess, bulk, Te is removed each cycle. Excess Te may build up at certain sites, which may then have better conductivity then the rest of the deposit, so that more Te is deposited at those sites in the next cycle, a self propagating system. This problem is most troublesome at the higher cycle numbers, where the particle growth appears to be exponential with the number of cycles, rather

that linear. A high defect density is expected for these deposits, based on the substrate, due to the severe lattice mismatch (~10%) between the Au and the CdTe, and the short terrace width of the Au surface. Strain caused by this mismatch and the stepped polycrystalline surface could be responsible for the Te nucleation sites.

The elemental stoichiometry and relative coverages were determined by EPMA. Absolute coverages by this technique cannot be determined as the thin films constitute only a small fraction of the probe beam's total sample volume. However, the Cd and Te signals are proportional to their coverages and the system was calibrated using a single crystal of CdTe. Figure 8 shows the relative Cd and Te coverages for the thin-films. The graph is linear throughout, consistent with layer-by-layer growth. In addition, the ratio of Cd to Te is 1 for all samples except the 1000 cycle film. It is has a ratio of 0.95, indicating a slight excess of Te within the film, consistent with the appearance of the Te clusters in Figure 7C.

Grazing incident angle XRD studies have also been performed. Angle between 0.2 and 0.5 degrees were used as most of the Au and Si reflections were eliminated. The incident angle was varied to maximize the CdTe reflections and minimize any substrate reflections. Figure 9 shows patterns for three deposits, each containing peaks consistent with cubic CdTe: the (111), (220) and (311) reflections are observed at 23.8°, 39.4°, and 46.5° respectively. The peak at 64.5° is a remnant of the (220) Au reflection. The relative sizes of the peaks clearly indicate a preference for the (111) plane of CdTe. Hexagonally orientated planes are expected, given the (111) surface texture of the Au substrates. The XRD of the 500 cycle sample, Figure 9B, shows the same cubic CdTe reflections as the 200 cycle sample (Figure 9A), however, the peak at 38.3° seem to indicate that small amounts of elemental Te are starting to form as a separate phase. By 1000 cycles (Figure 9C), a separate Te phase is evident at 27.6°, 38.3°, 40.5°, 46.0°, 49.6° (the (101), (102), (110), (003), and (201) reflections respectively) and a decrease in the quality of the CdTe signal is

also seen. Again, it is evident that the deposit is not ideal and that Te clusters are becoming a primary component of the films.

CdSe Thin-Films

Unlike CdTe, little work has been done on the electrochemical ALE of CdSe thin-films, and as a result, uniform deposits are more difficult to achieve. Initially, a two step deposition process for Se was utilized, where bulk Se was deposited at -0.6 V and stripped at -0.8 V. A pH 4.5 $HSeO_3^-$ solution was used. Cd was deposited at -0.55 V. Under those conditions, only red powdery films, consisting mostly of elemental Se were produced. This red Se is characteristic of Se deposited by conproportionation [37]. Unfortunately, Se electrochemistry has been found to be extremely complicated and is not yet fully understood [38]; however, it is apparent that the system is quite sensitive to pH and Se concentration [38, 39]. Thus, a second Se solution, pH 9.2, was tried and found to shift the peak potential for *reductive* deposition of a Se atomic layer to -0.6 V. As a result, a new ECALE cycle was created, using two *reductive* "UPD" processes. The CdSe cycle used potentials of -0.6 V for Cd UPD and -0.9 V for Se "UPD"; the Se stripping step was removed. Se "UPD" was performed at -0.9 V in this solution, as it appeared to allow completion of the atomic layer, but avoided significant bulk deposition. The quotation marks are used on Se "UPD" because of the irreversibility of the atomic layer deposition process. That is, the atomic layer is really deposited at an overpotential.

Like with CdTe, a series of deposits were made (50 to 1000 cycles). The resulting deposits were similar in appearance to the CdTe films. The deposits appeared brown after 50, pink after 100, gray blue after 150, gold green after 200, pink gold after 500, and black after 1000 cycles. Films made with 500 cycles or less were very smooth and shiny in appearance, but the 1000 cycles film was opaque and nonreflective.

SEM micrographs of 200, 500, and 1000 cycle CdSe deposits (Figure 10) exhibit small crystallites. The crystallites grew in size with increasing numbers of cycles. By 1000 cycles, the crystallites roughened the surface sufficiently to diffusely scatter light, giving the films an opaque

appearance. The crystallites are significantly different in appearance than the particles observed on the CdTe films. This appears to be due to the chalcogenide deposition step. In CdTe formation, the Te was first deposited as bulk, and (as discussed previously) it appears that the stripping step was insufficient to completely reduce all of the excess bulk Te, resulting in the gradual accumulation of small Te crystallites on the surface. In CdSe formation, Se deposition was achieved using a single step in a process which appears more surface limited, and avoids the build up of chalcogenide, and the resulting particles.

The relative coverages of Cd and Se as a function of the number of cycles are diagramed in Figure 11. The graph is similar to that for CdTe, its linearity is, again, consistent with layer-by-layer growth. On average, the deposits appear a little rich in Se, as much as 12% for the 500 cycle deposit. This problem with the stoichiometry might be expected, considering the minimal work done to optimize these deposits, compared with CdTe.

Comparison of the Cd signal for the CdSe films and the CdTe films suggest that the CdSe films are twice as thick as the CdTe films, for the same number of cycles. The Cd deposition potentials used to make both sets of films, were the same. However, CdSe is thermodynamically more stable than CdTe, suggesting that, all else being equal, the potential needed for Cd UPD to form CdSe should be more positive then that needed to form CdTe. There are larger numbers of variables in the cycles for the deposition of both compounds [27], making this kind of direct comparison dangerous. A second explanation for the increased coverage observed with CdSe involves the lattice match with the Au substrate. The lattice parameters of CdSe and Au are only 0.6% apart, greatly decreasing any lattice strain, and possibly facilitating the formation of more complete monolayers each cycle [40-44].

Figure 12 shows XRD patterns for 200 cycle deposits of CdTe, CdSe, and CdS. CdSe is similar to CdTe in that it is a cubic film, as determined by the (111), (220), and (311) reflections at 25.3°, 42.0°, and 49.7°, respectively. The peak at 64.4° is, again, a remnant of the (220) Au reflection. The relative intensities of the three peaks, again, indicates that the (111) orientation is

preferred. XRD patterns were also obtained from each of the CdSe deposits used to form Figure 11. Unlike the XRD pattern shown in Figures 9B and C, where traces of the elemental chalcogenide were visible, no evidence for elemental Se is observed for the CdSe deposits, even though they were somewhat rich in Se (Figure 11). Again, this can be traced back to the method of chalcogenide deposition, since no bulk Se is deposited, no separate phase should be observed.

Comparing the (111) peaks for CdSe and CdTe in Figure 11, it appears that the CdSe peak is nearly twice the size as that for CdTe. This is consistent with the EPMA results discussed above, where it was concluded that there was probably twice as much CdSe after 200 cycles, as there was CdTe. Recent measurements of the absolute amounts of Cd using inductively coupled plasma – mass spectrometry have shown this to be the case. Those results indicate that the coverage of CdTe is about 0.4 ML/cycle, were as the CdSe is more like 0.8 ML/cycle. That is the CdSe is much closer to being the ideal 1 ML/cycle that we expect.

CdS Thin-Films

The first attempts to form CdS thin films with more than 5 cycles utilized -0.6V for both Cd and S deposition. The resulting films were uniform and light yellow in color. EPMA analysis, however, showed them to be approximately 20% high in S. In the ECALE program, the S^{2-} species were exposed to the substrate at open circuit; however, unlike the Te^{+4} and Se^{+4} species, S^{-2} appears to undergo some uncontrolled spontaneous deposition, onto either the Au or Cd coated surfaces, at open circuit [28], possibly accounting for the excess of S.

The next series of CdS deposits were made by rinsing in the S^{2-} species at a controlled potential of -0.8V, instead of at open circuit, to prevent the spontaneous deposition of S, hopefully limiting the amount of S deposited on the surface. A series CdS films were made using this program, and 25 to 200 cycles. The films became increasingly yellow as the film's thickness increased. However, unlike the CdTe and CdSe films, no color changes were observed. A graph of the relative coverages of Cd and S versus the number of cycles is shown in Figure 13. Again, layer-by-layer growth is supported by the linear relationship observed. Comparison of the Cd

signal from the 200 cycle CdTe and CdS films, suggest that the CdS films are half as thick as the CdTe films, possibly 0.2 ML/cycle. It is unclear why these films should be so much thinner, as CdS is the most thermodynamically stable of the three Cd chalcogenide compounds. In addition, the lattice mismatch with gold is small (~2.5%). The Cd/S ratio (Figure 14) decreases from a maximum of 1.13 to a minimum of 0.9 as the number of cycles increases. The decline in the Cd/S ratio could be an indication that deposition conditions should be adjusted as the films grow in thickness. However, given that so little work has been done so far to optimize the CdS ECALE cycle, the low relative coverages are difficult to interpret.

Figure 12C is the XRD spectra for a 200 CdS cycle film. Like CdTe and CdSe films, it is cubic with a preferred (111) orientation. The (111), (220), and (311) reflections are observed at 26.5°, 43.9°, and 52.1°, respectively. The CdS (111) peak has a significantly lower signal to noise then CdTe and CdSe, possibly indicating a lower quality of film, compared with those of CdTe or CdSe (Figure 12A and 12B, respectively).

Conclusions

An automated electrochemical deposition system has been constructed and used to form cubic thin-films of CdTe, CdSe, and CdS with predominate (111) orientations, using the ECALE methodology. Significant improvements in deposit morphology and quality were achieved by switching from a thin-layer cell to a thick-layer H-cell. Films formed with 200 or less cycles generally show a smooth morphology; however, deposits made with 500 or more cycles showed increased amounts of particulates or crystallites. The parameters used were, in general, determined using a thin layer electrochemical cell, not the cell used to form the deposits. It is expected that the deposit morphology for the thicker films will improve with more work, optimizing parameters with the new electrochemical cells. In addition, the Au coated Si substrates are a large improvement over deposits formed on Au foil, however, they still provide numerous nucleation sites due to their polycrystalline nature.

Figures

Figure 1: Diagrams of thin-layer flowcell face plates. Inlet and outlet ports are 1/4-28 tapped which then reduce to a 0.010 in. solution channel. The Vicor plug has been fitted into 1/8 in hole drilled into a 1/4-28 PEEK flangless nut. (A) The Vicor plug is located above the working electrode flush with the inside face of the flowcell. (B) The Vicor plug has been tapped into the outlet solution channel.

Figure 2: Pictured is the effect of a bubble on a CdTe thin film made with a thin-layer flowcell (magnification of 250). An outline of a bubble's edge is seen on the left with a tail of particulates flowing away (towards the outlet).

Figure 3: Diagram of a modified H-cell, six way selection valve and sample holder.

Figure 4: Diagram of the automated electrochemical deposition system.

Figure 5: Diagram of an ECALE cycle for CdTe formation. Top half represents the solution pumping scheme. Small squares represent a single rinse of solution into and out of the cell. A dashed edge on a box indicates that the solution still resides in the cell. Blocks with numbers indicate deposition times. Lower half represents the potential control scheme.

Figure 6: FESEM micrographs of A) clean substrate before deposition and (B) after 200 CdTe ECALE cycles.

Figure 7: SEM micrographs of CdTe thin films. (A) 200 ECALE cycles, (B) 500 ECALE cycles, (C) 1000 ECALE cycles.

Figure 8: A plot of relative coverage as a function of the number of CdTe ECALE cycles as determined by EPMA.

Figure 9: Glancing angle XRD of CdTe thin films formed by (A) 200 ECALE cycles, (B) 500 ECALE cycles, and (C)1000 ECALE cycles.

Figure 10: SEM micrographs of CdSe thin films. (A) 200 ECALE cycles, (B) 500 ECALE cycles, (C) 1000 ECALE cycles.

Figure 11: A plot of relative coverage as a function of the number of CdSe ECALE cycles as determined by EPMA.

Figure 12: Glancing-angle XRD of 200 ECALE cycles of (A) CdTe, (B) CdSe, and (C) CdS.

Figure 13 A plot of relative coverage as a function of the number of CdS ECALE cycles as determined by EPMA.

Figure 14: A plot of the Cd/S ratio as a function of the number of CdS ECALE cycles as determined by EPMA.

1. Z. Loizos, A. Mitsis, N. Spyrellis, M. Froment, and G. Maurin, Thin Solid Films 235:51 (1993).

2. R. B. Gore, R. K. Pandey, and S. K. Kulkarni, J. Appl. Phys. 65:2693 (1989).

3. J. Ortega, Anales de Quimica 87:641 (1991).

4. G. F. Fulop and R. M. Taylor, Ann. Rev. Mater. Sci. 15:197 (1985).

5. G. Hodes, in "Physical Electrochemistry" (I. Rubinstein, ed.), 1995, p. 515.

6. R. K. Pandey, S. N. Sahu, and S. Chandra, Handbook of Semiconductor Electrodeposition, Marcel Dekker, Inc., New York, 1996.

7. B. W. Gregory and J. L. Stickney, J. Electroanal. Chem. 300:543 (1991).

8. R. C. DeMattei and R. S. Feigelson, in Electrochemistry of Semiconductors and Electronics, Processes and Devices (J. McHardy and F. Ludwig, eds.), Noyes Publications, Park Ridge, NJ, 1992, p. 1.

9. E. A. Dalchiele and S. Bonilla, J. Braz. Chem. Soc. 3:95 (1992).

10. G. C. Morris and R. J. V. d. Veen, Sol. Energy Mat. Sol. Cells 30:339 (1993).

11. K. Rajeshwar, Adv. Mater. 4:23 (1992).

12. J. Dutta, D. Bhattacharyya, A. B. Maitil, S. Chaudhuri, and A. K. Pal, Vacuum 46:17 (1995).

13. G. Hodes, J. Manassen, and D. Cahen, Nature 261:403 (1976).

14. M. P. R. Panicker, M. Knaster, and F. A. Kroger, J. Electrochem. Soc. 125:566 (1978).

15. J. M. Fisher, L. E. A. Berlouis, B. N. Rospendowski, P. J. Hall, and M. G. Astles, Semiconductor Science and Technology 8:1459 (1993).

16. C. Wei, N. Myung, and K. Rajeshwar, J. Electroanal. Chem. 347:223 (1993).

17. S. M. So, W. Hwang, P. V. Meyers, and C. H. Liu, J. Appl. Phys. 61:2234 (1987).

18. Y. Guo and X. Deng, Sol. Energy Sol. Cells 29:115 (1993).

19. Suntula, T., Anson, and J., , United States, 1977.

20. C. H. L. Goodman and M. V. Pessa, JAP 60:R65 (1986).

21. Kuech, T.F., Dapkus, P.D., Aoyagi, and Y., eds., Atomic Layer Growth and Processing, Vol. 222, Materials Research Society, Pittsburgh, 1991.

22. Bedair and S., eds., Atomic Layer Epitaxy, Elsevier, Amsterdam, 1993.

23. B. W. Gregory, M. L. Norton, and J. L. Stickney, J. Electroanal. Chem. 293:85 (1990).

24. Kolb and D.M., , Vol. 11 (H. Gerischer and C. W. Tobias, eds.), Wiley, New York, 1978, p. 125.

25. R. R. Adzic, in Advances in Electrochemistry and Electrochemical Engineering, Vol. 13 (H. Gerishcher and C. W. Tobias, eds.), Wiley-Interscience, New York, 1984, p. 159.

26. B. M. Huang, L. P. Colletti, B. W. Gregory, J. L. Anderson, and J. L. Stickney, J. Electrochem. Soc. 142:3007 (1995).

27. L. P. Colletti and J. L. Stickney, (in prep).

28. L. P. Colletti, D. Teklay, and J. L. Stickney, J. Electroanal. Chem. 369:145 (1994).

29. L. P. Colletti, S. Thomas, E. M. Willmer, and J. L. Stickney, in Electrochemical Synthesis and Modification of Materials (P. C. Searson, T. P. Moffat, P. C. Andricacos, S. G. Corcoran, and J. L. Delplancke, eds.), Materials Research Society, Pittsburgh, 1996.

30. J. W. Schultze, F. D. Koppitz, and M. M. Lohrengel, Ber. Buns. Phys. Chem. 78:693 (1974).

31. F. M. Romeo, R. I. Tucceri, and D. Posadas, SS 203:186 (1988).

32. M. R. Deakin and O. Melroy, JEC 239:321 (1988).

33. J. C. Bondos, A. A. Gewirth, and R. G. Nuzzo, Journal of Physical Chemistry 100:8617 (1996).

34. A. N. Buckley, I. C. Hamilton, and R.Woods, JEC 216:213 (1987).

35. I. C. Hamilton and R. Woods, JAE 13:783 (1983).

36. G. Maurin and D. Pottier, J. Mater. Sci. Lett. 6:817 (1987).

37. M. D. Vazquez and P. S. Batanero, Electrochim. Acta 37:1165 (1992).

38. C. Wei, N. Myung, and K. Rajeshwar, JEC 375:109 (1994).

39. G. S. R. Rao and J. J. Reddy, Acta Chim. Hung. 118:241 (1985).

40. T. E. Lister and J. L. Stickney, Applied Surface Science (1996).

41. T. E. Lister and J. L. Stickney, IJC accepted (1997).

42. Y. Golan, L. Vargulis, I. Rubinstein, and G. Hodes, Langmuir 8:749 (1992).

43. G. Hodes, Isr. J. Chem. 3:95 (1993).

44. Y. Golan, L. Margulis, G. Hodes, I. Rubinstein, and J. L. Hutchison, Surface Science 311:L633 (1994).

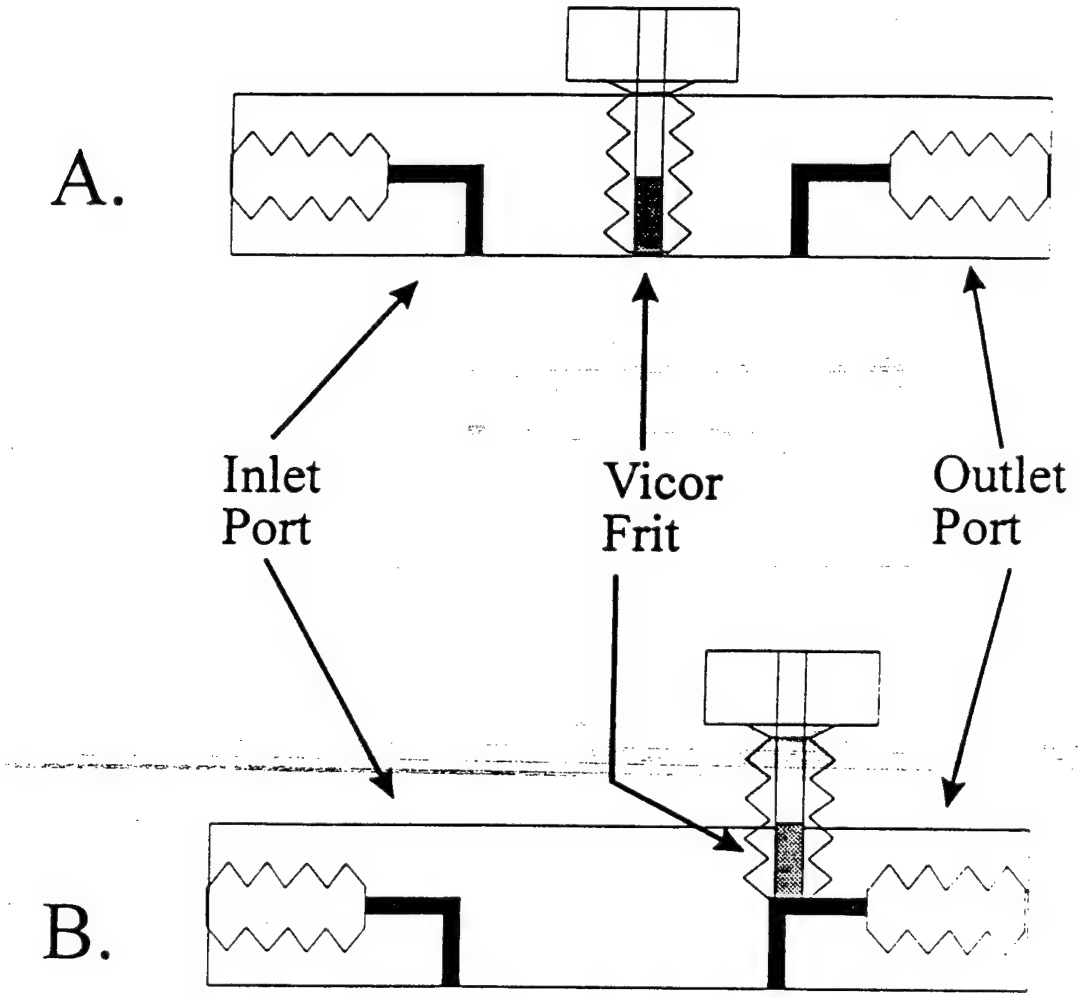
A.
Inlet
Port
Vicor
Frit
Outlet
Port
B.

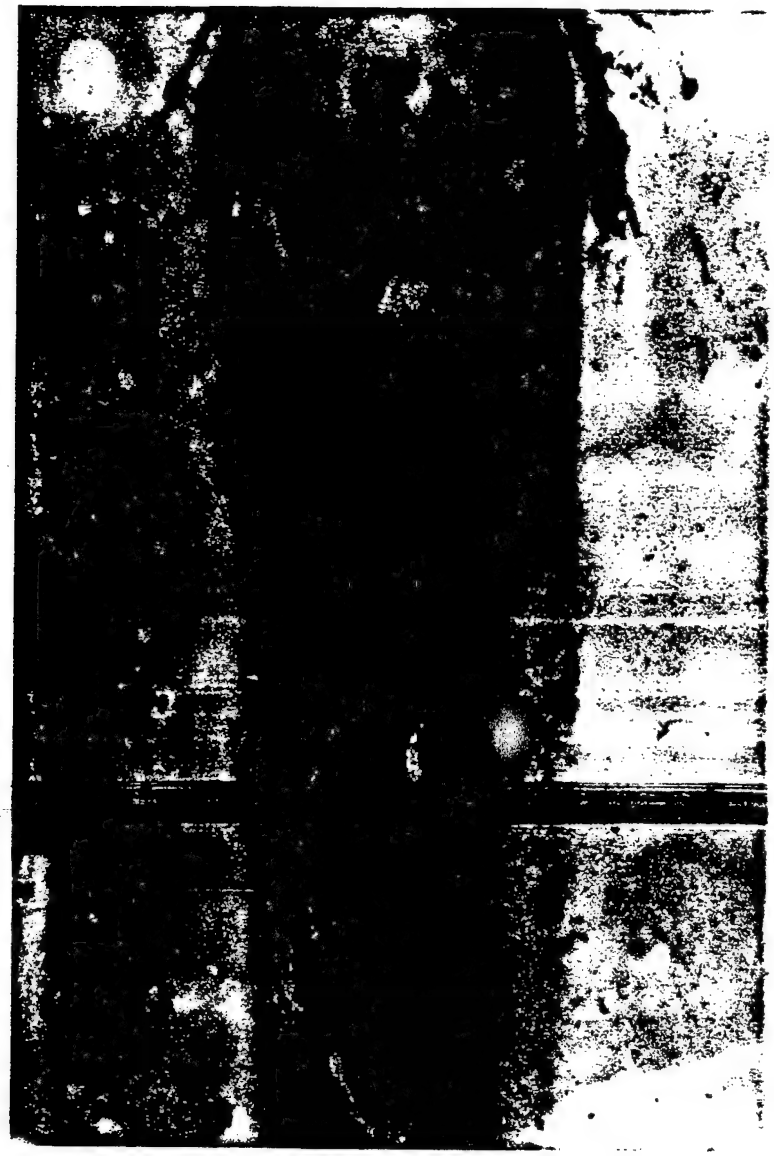

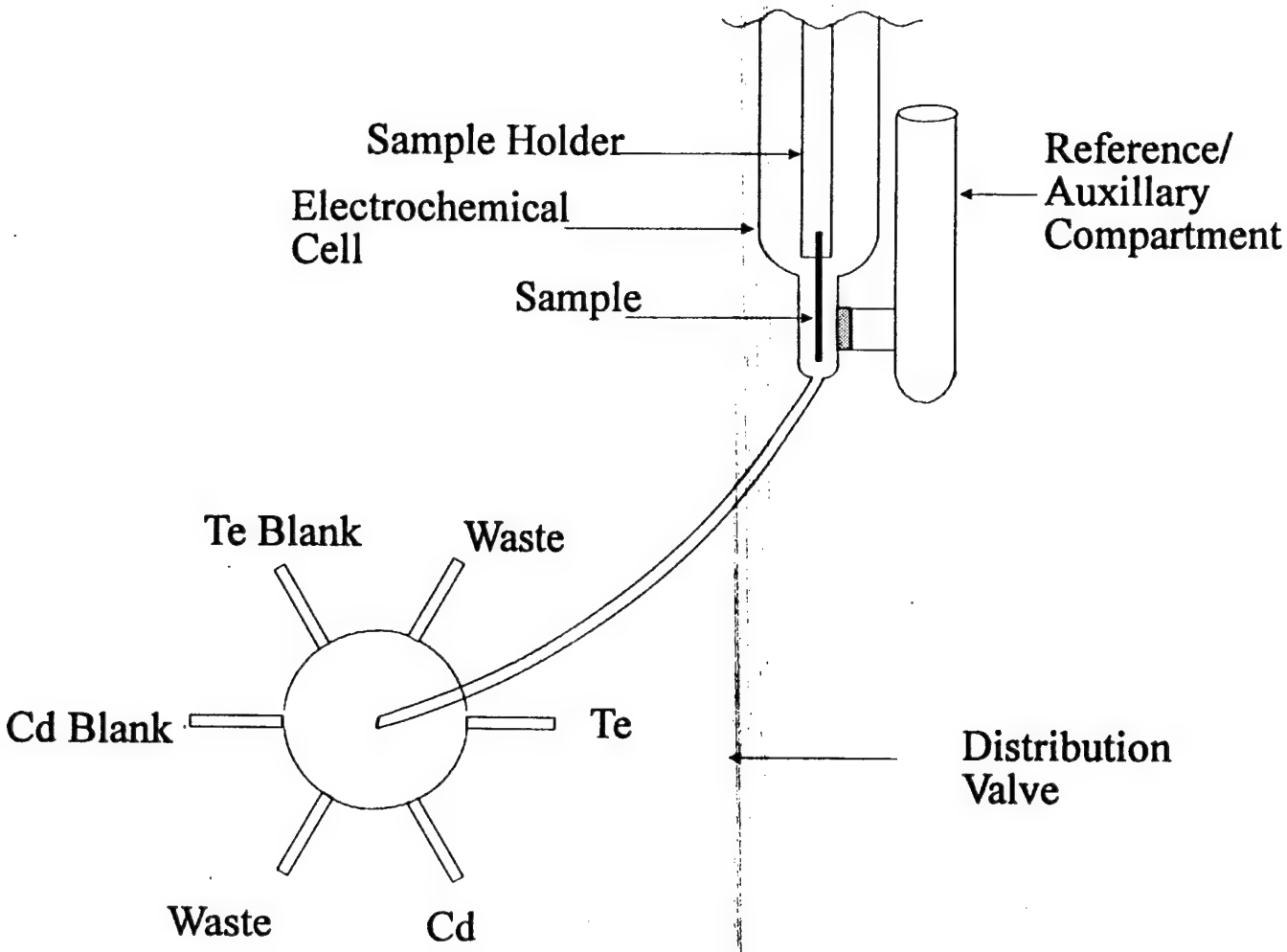
Sample Holder
Electrochemical Cell
Sample
Reference/ Auxillary Compartment
Te Blank
Waste
Cd Blank
Te
Waste
Cd
Distribution Valve

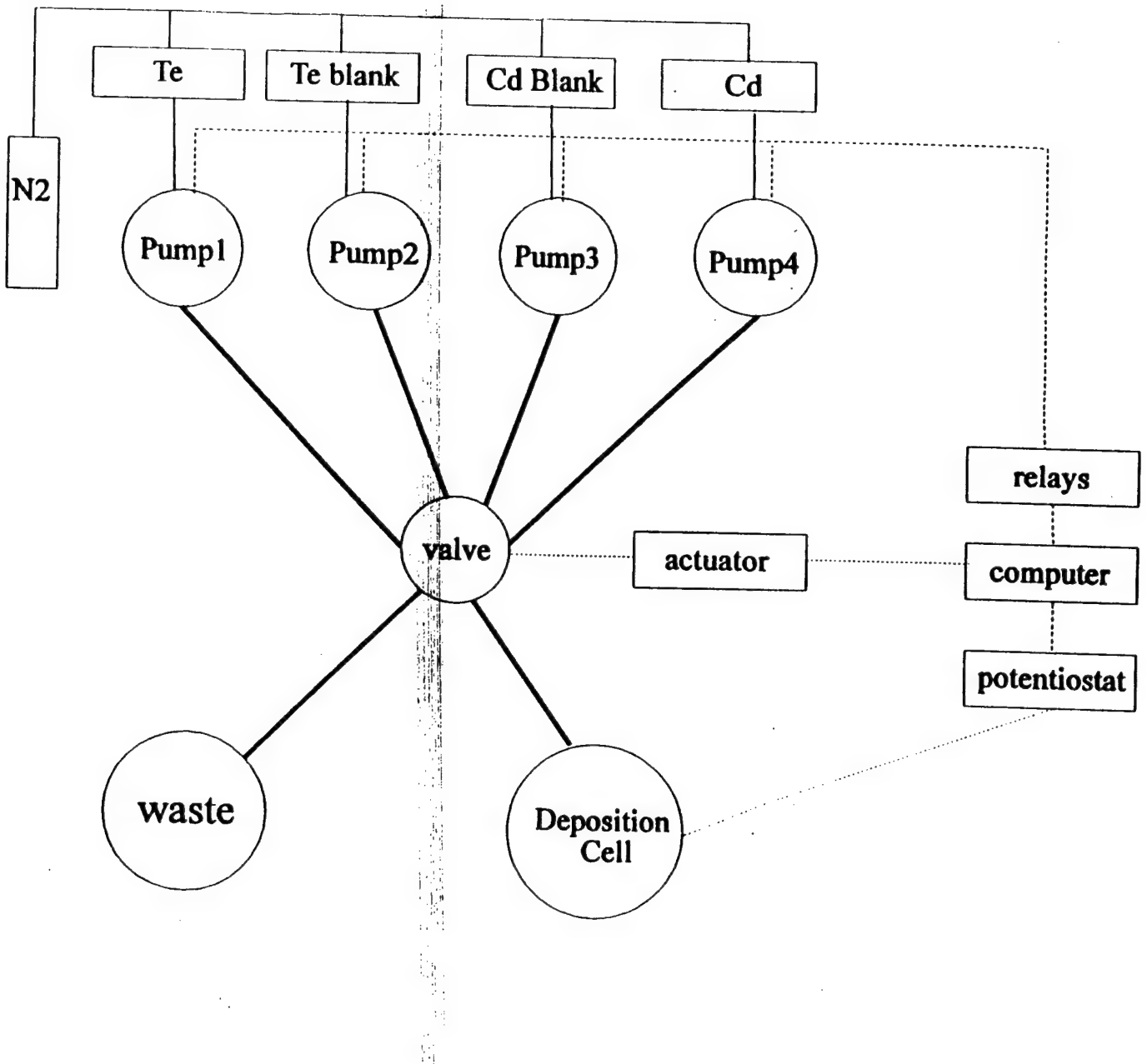
Te
Te blank
Cd Blank
Cd
N2
Pump1
Pump2
Pump3
Pump4
relays
valve
actuator
computer
potentiostat
waste
Deposition Cell

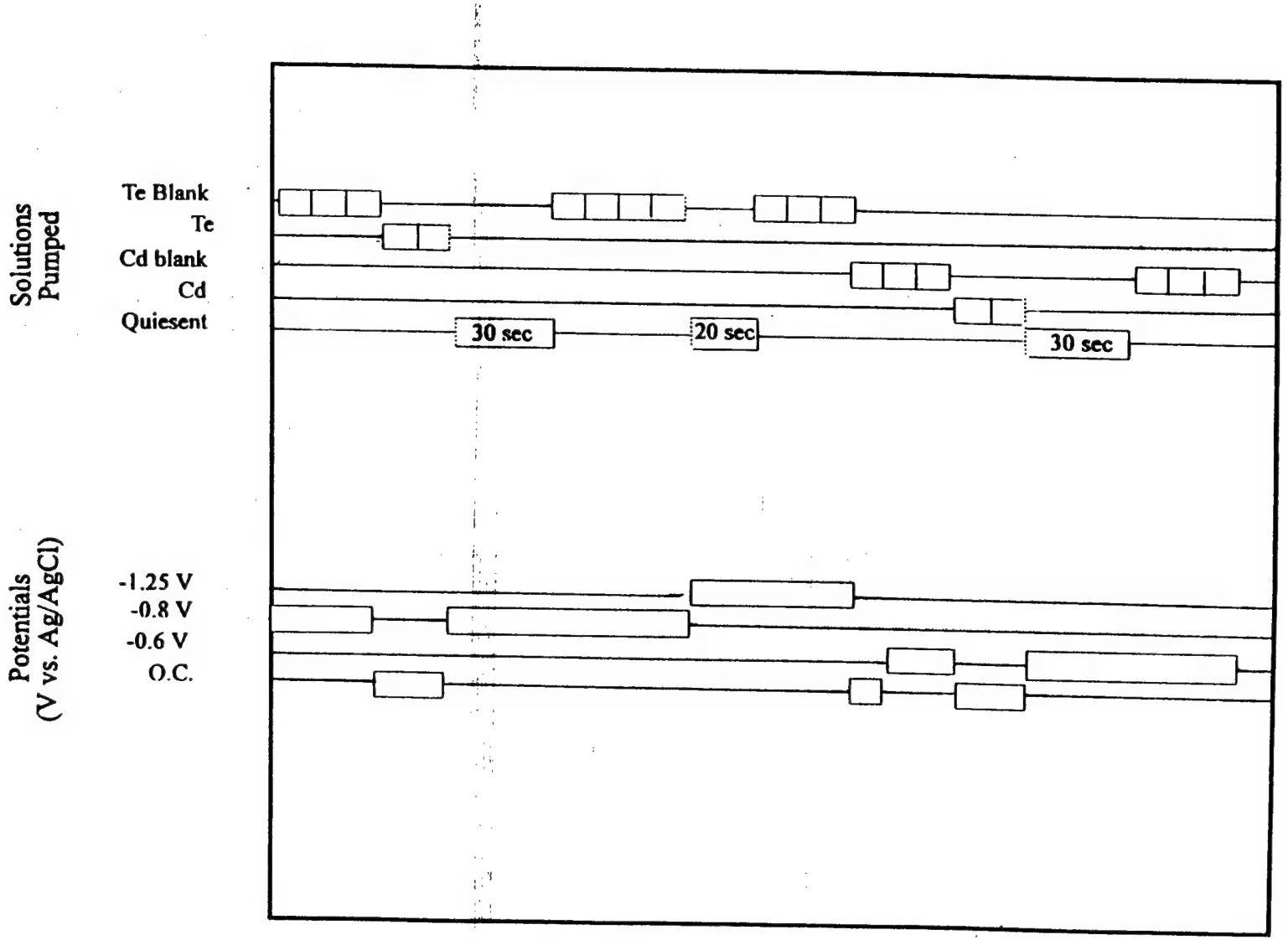
Solutions Pumped
Te Blank
Te
Cd blank
Cd
Quiesent
30 sec
20 sec
30 sec
Potentials (V vs. Ag/AgCl)
-1.25 V
-0.8 V
-0.6 V
O.C.

A.

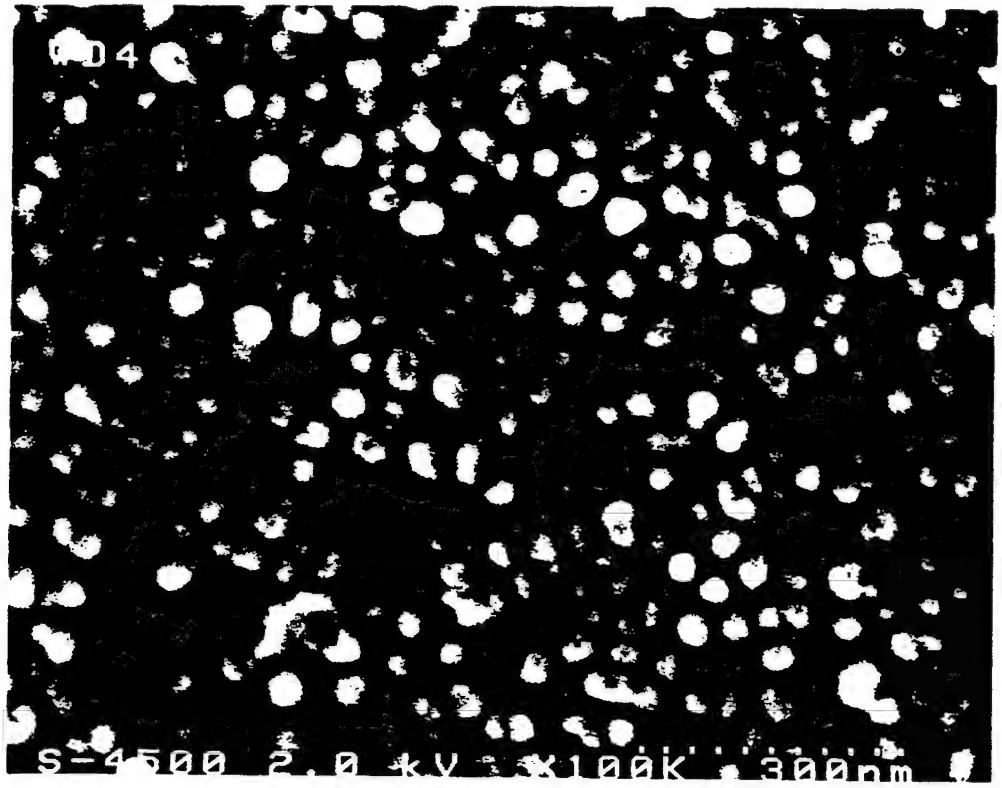

B.

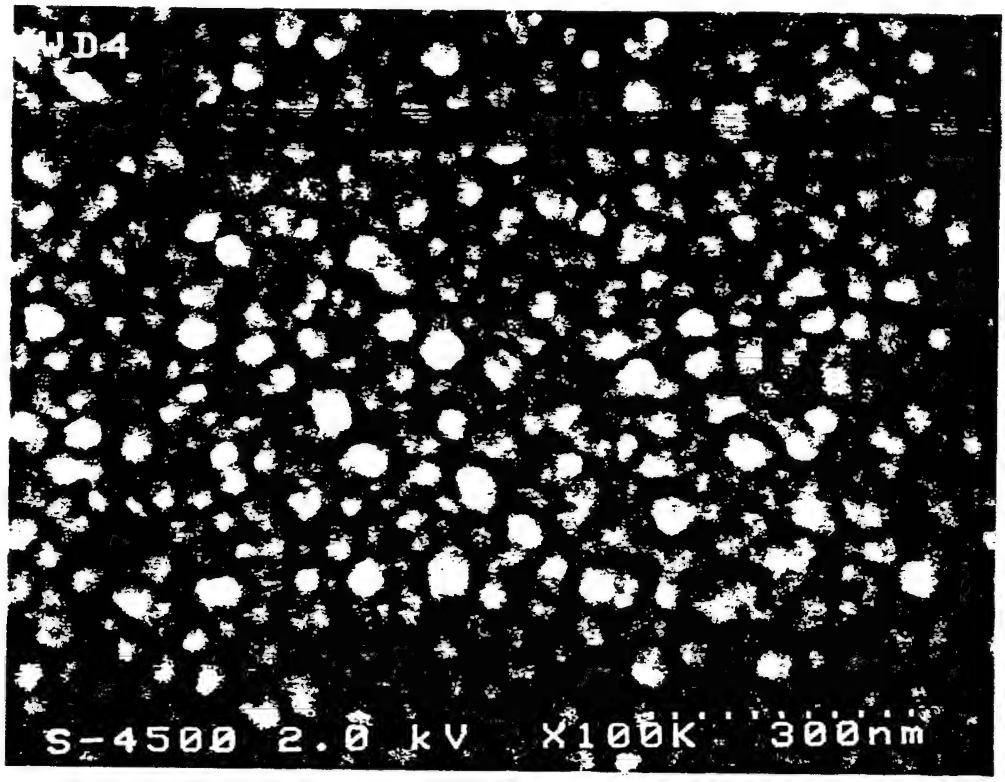

A.

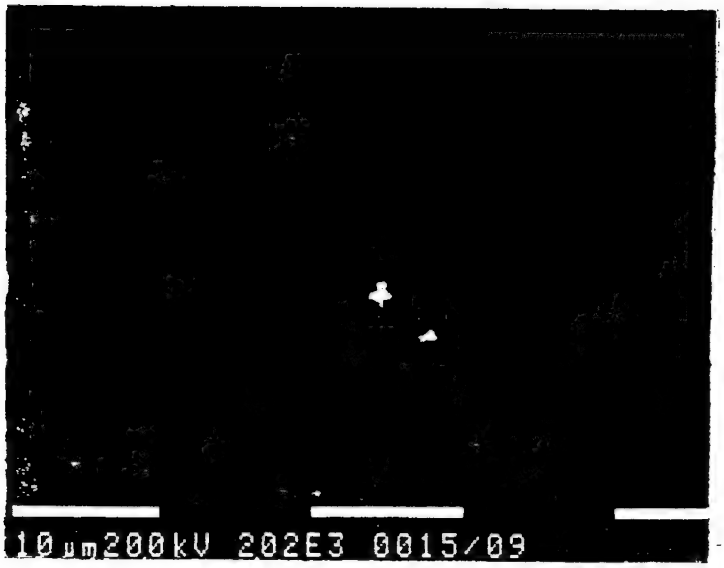

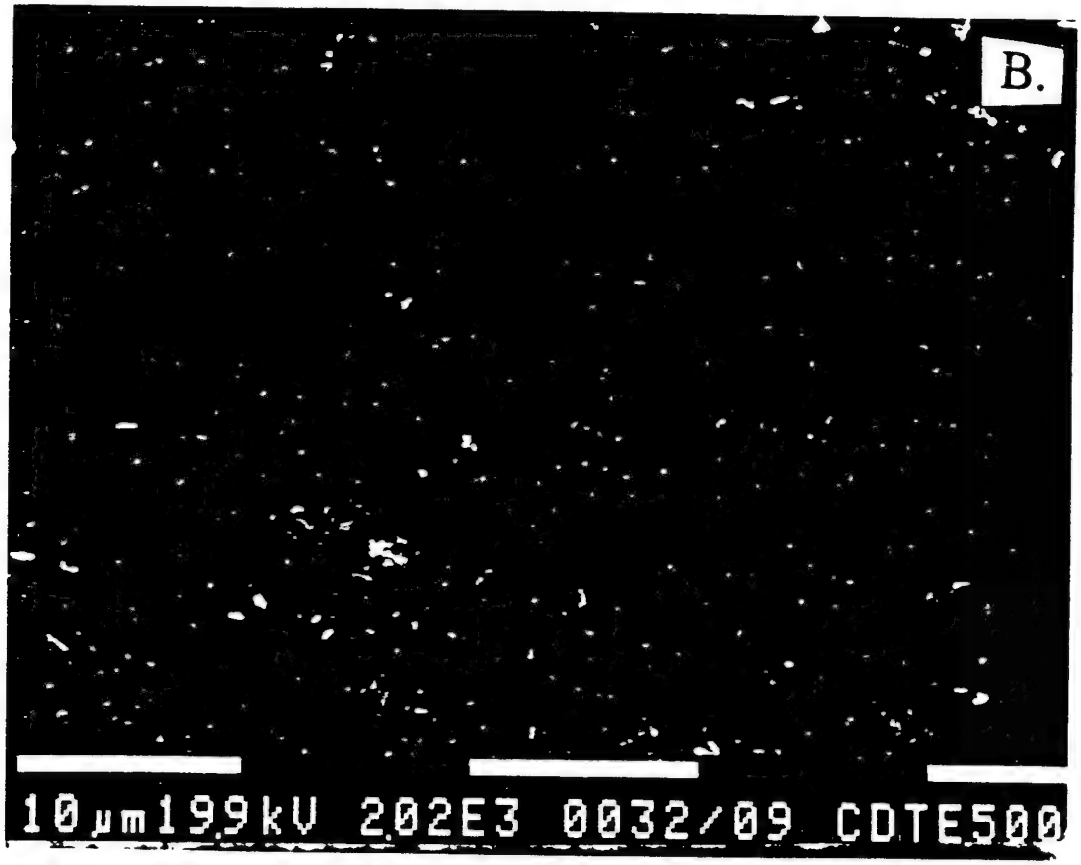
B.
10µm19.9kV 2.02E3 0032/09 CDTE500

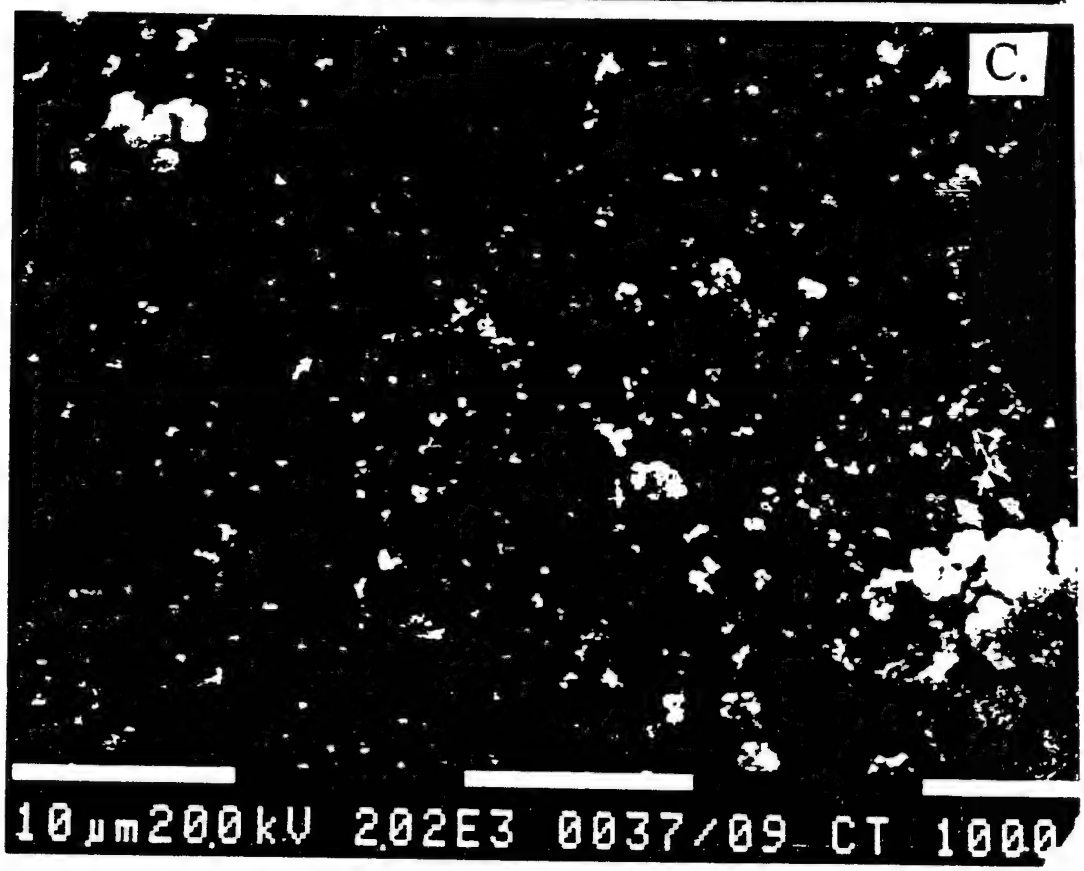
C.
10µm20.0kV 2.02E3 0037/09 CT 1000

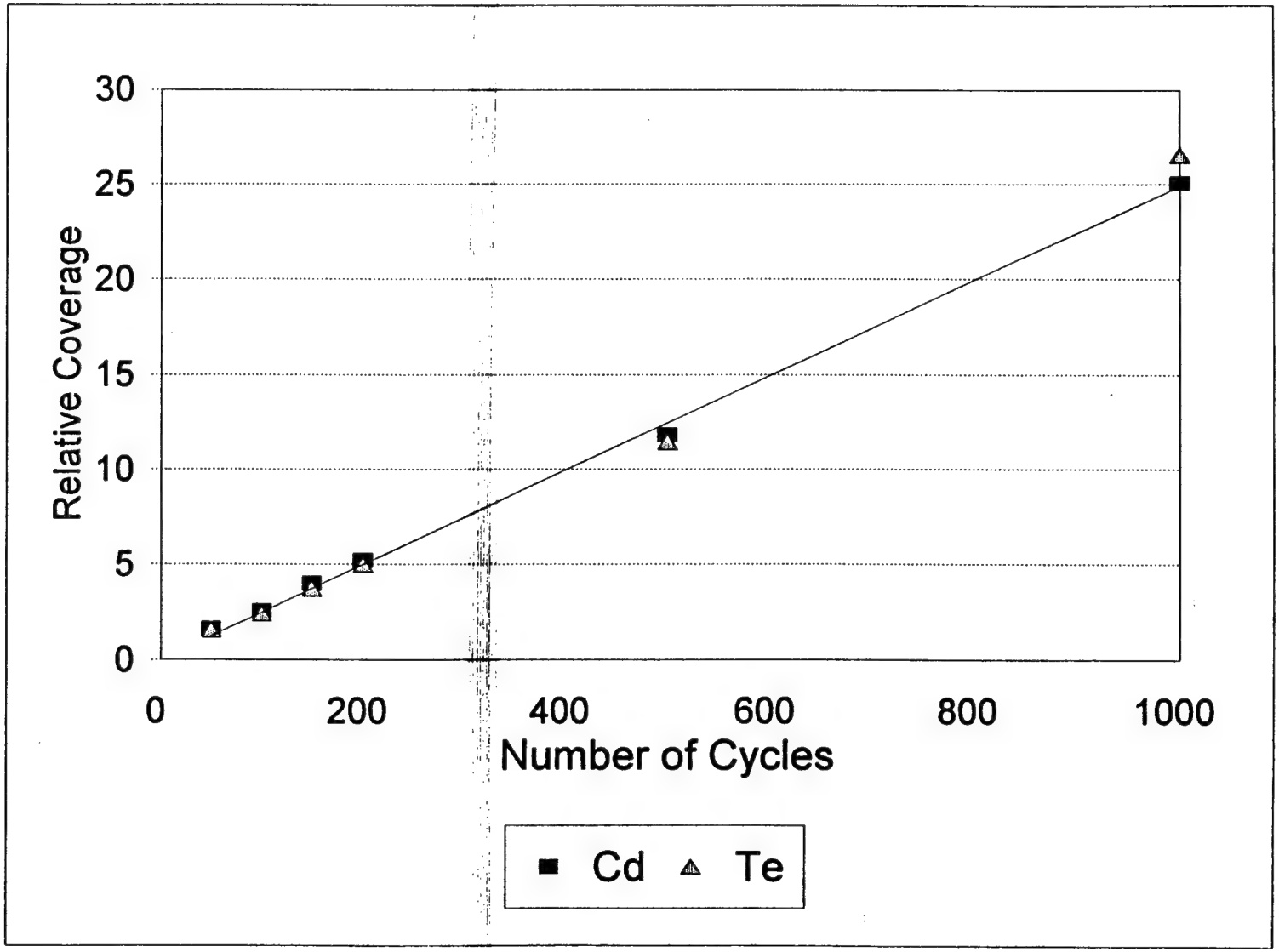
30
25
20
15
10
5
0
Relative Coverage
0
200
400
600
800
1000
Number of Cycles
Cd
Te

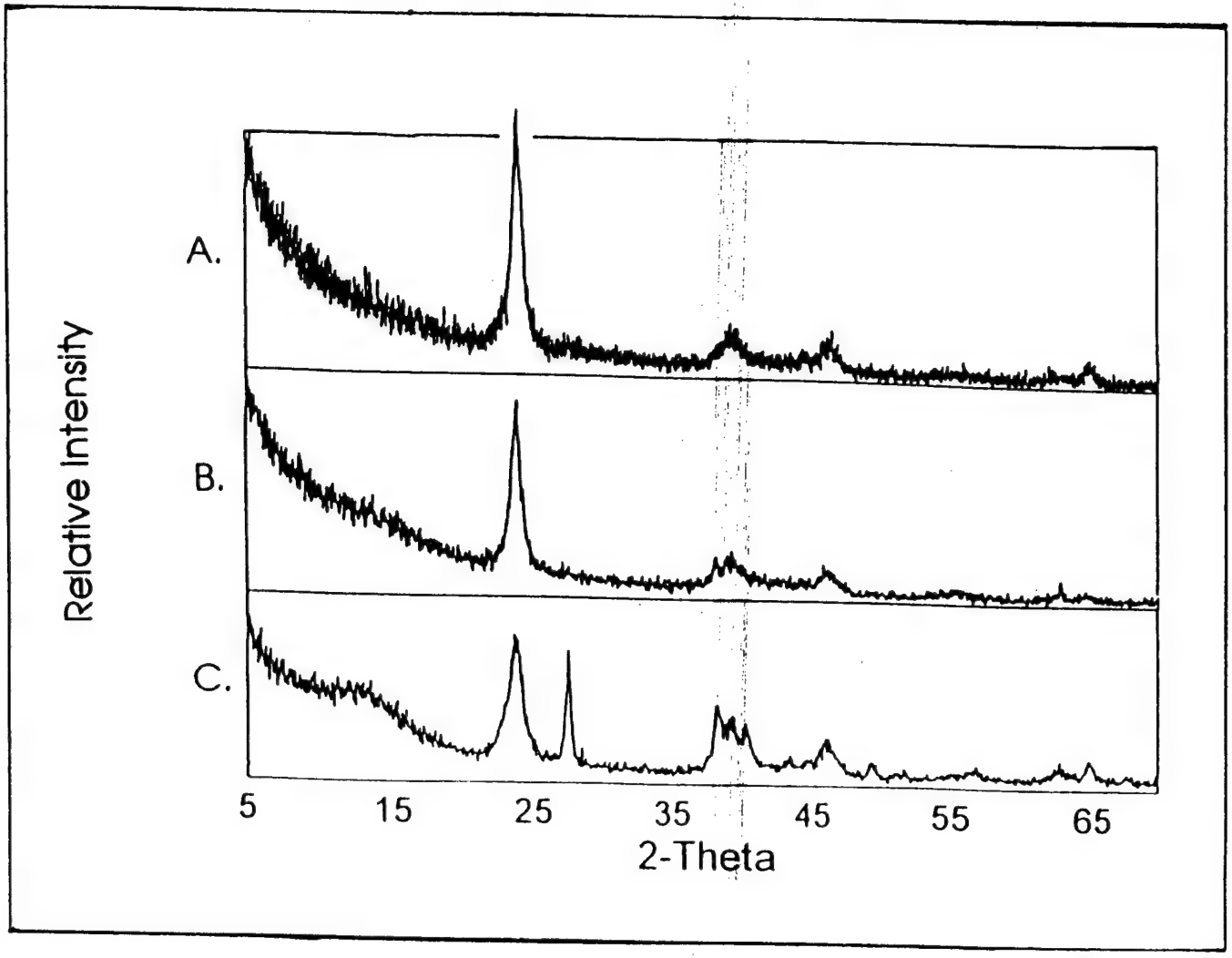
Relative Intensity
A.
B.
C.
5
15
25
35
45
55
65
2-Theta

A.

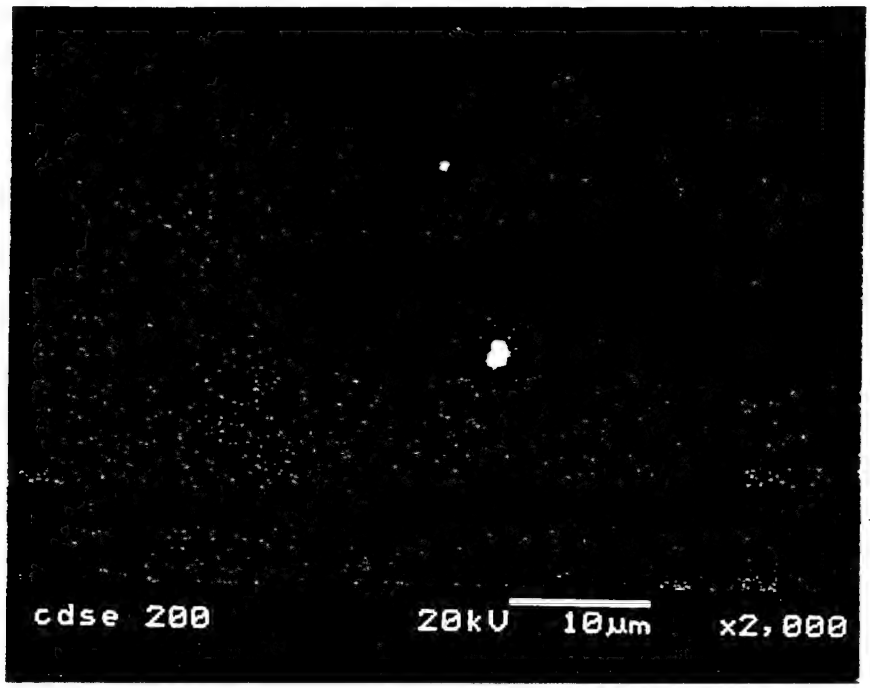

B.

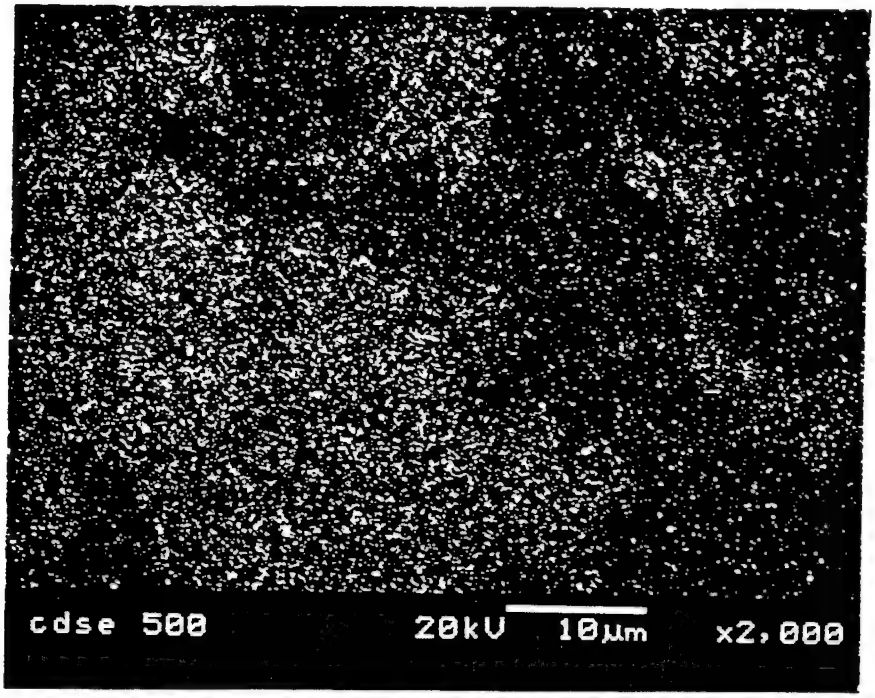

C.

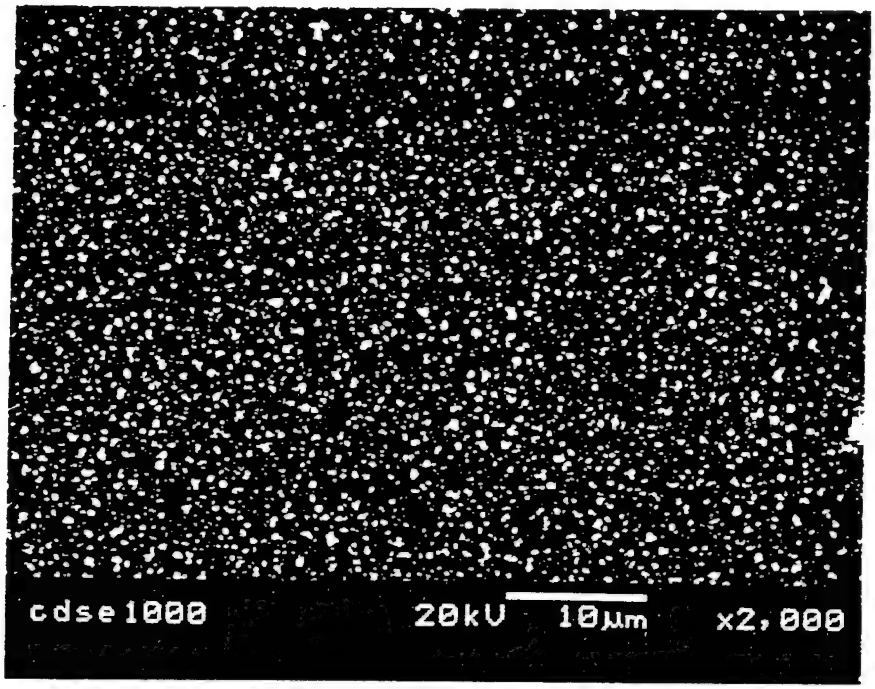

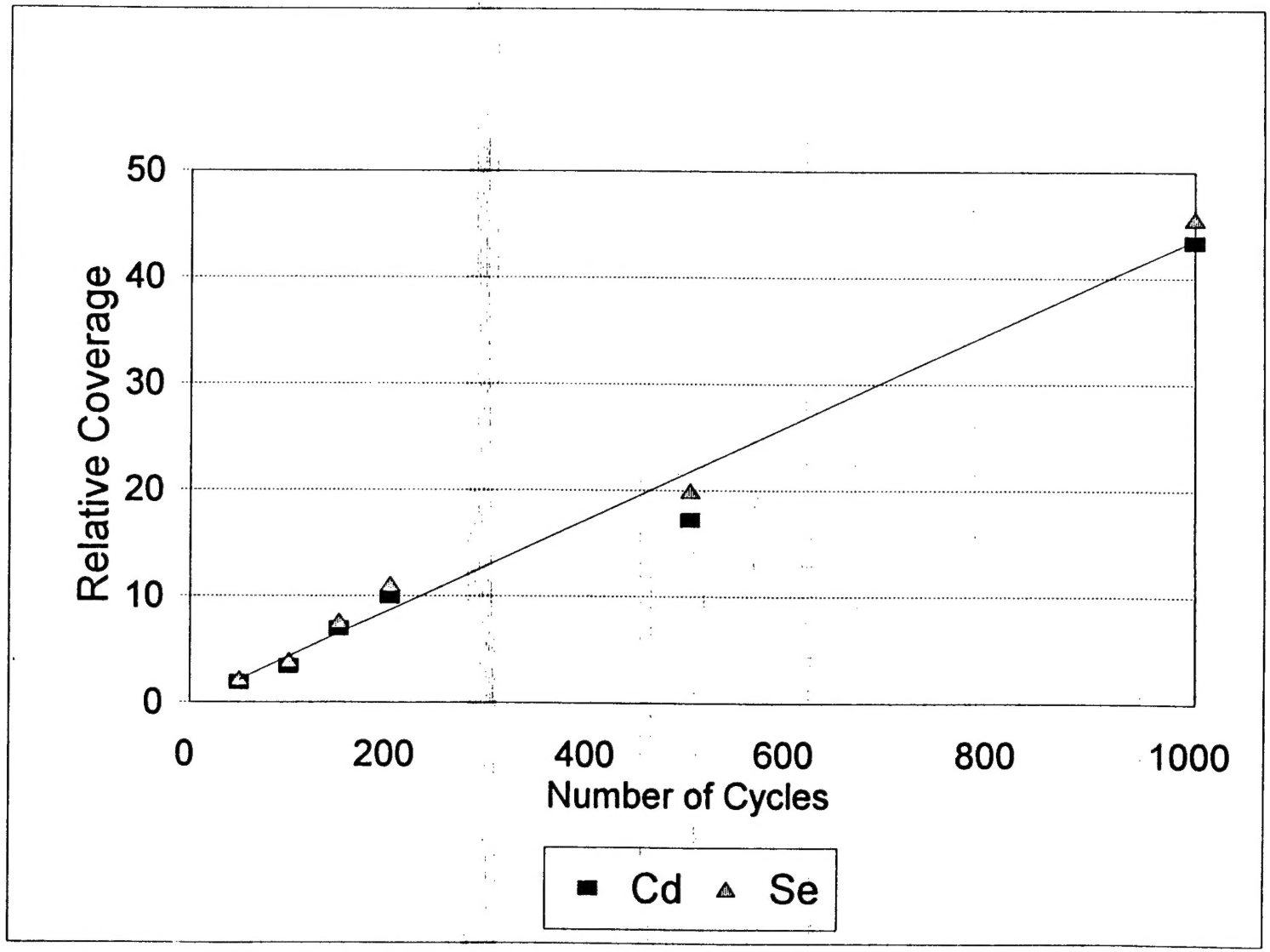
50
40
30
20
10
0
Relative Coverage
0
200
400
600
800
1000
Number of Cycles
Cd
Se

XRD of Cd II-IV Compounds

Omega optimized

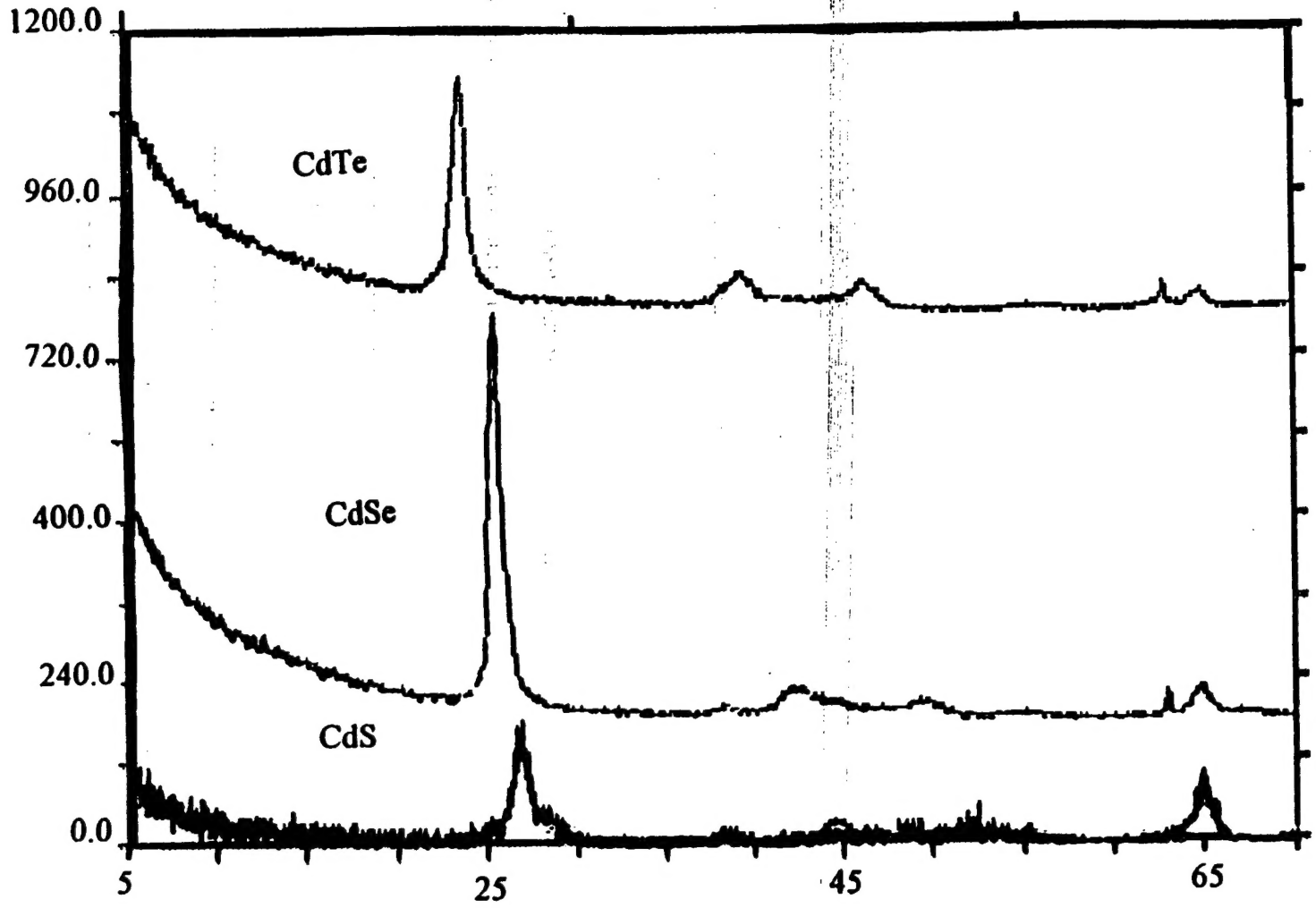

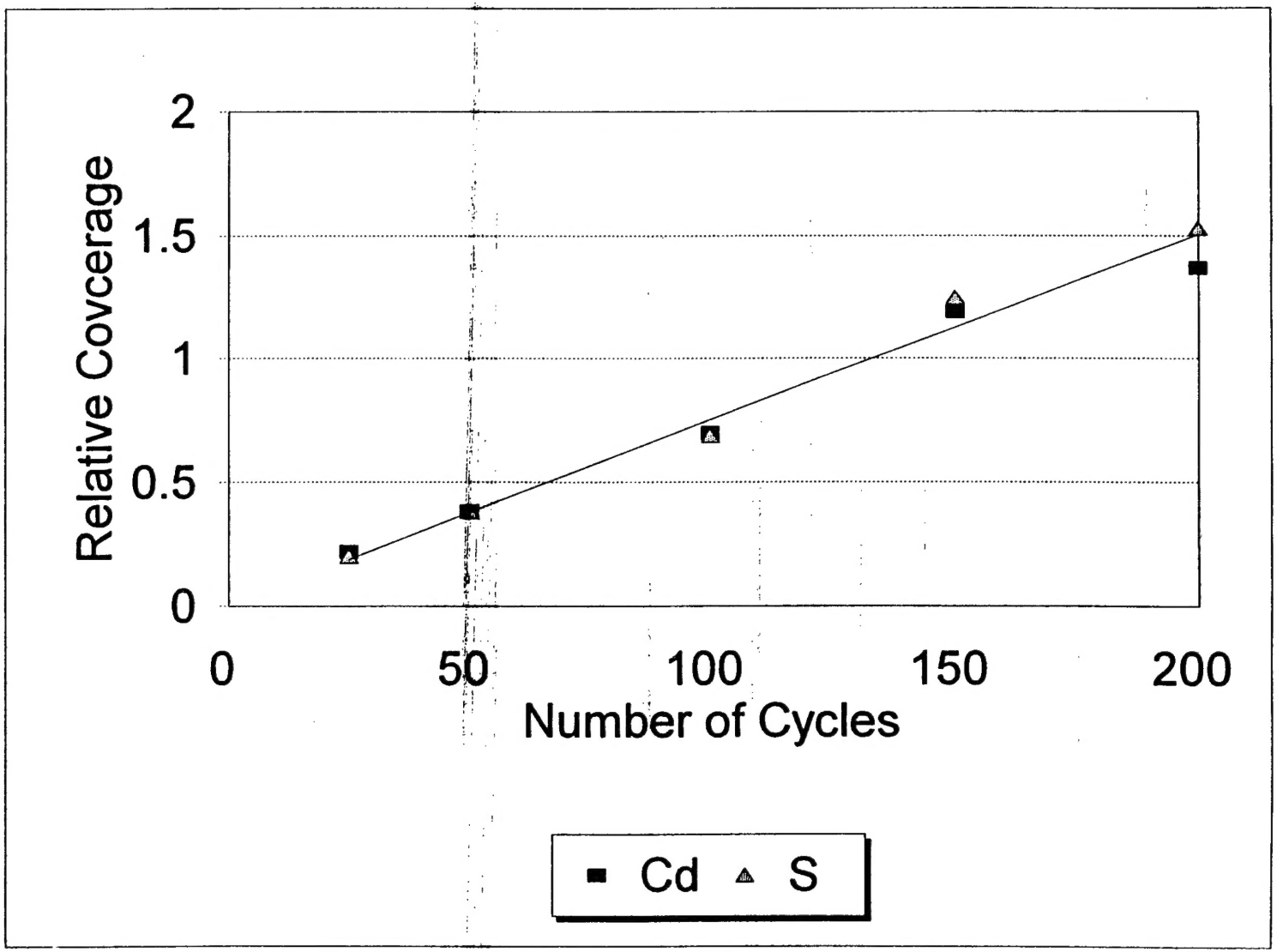
Relative Covcerage
2
1.5
1
0.5
0
0
50
100
150
200
Number of Cycles
Cd
S

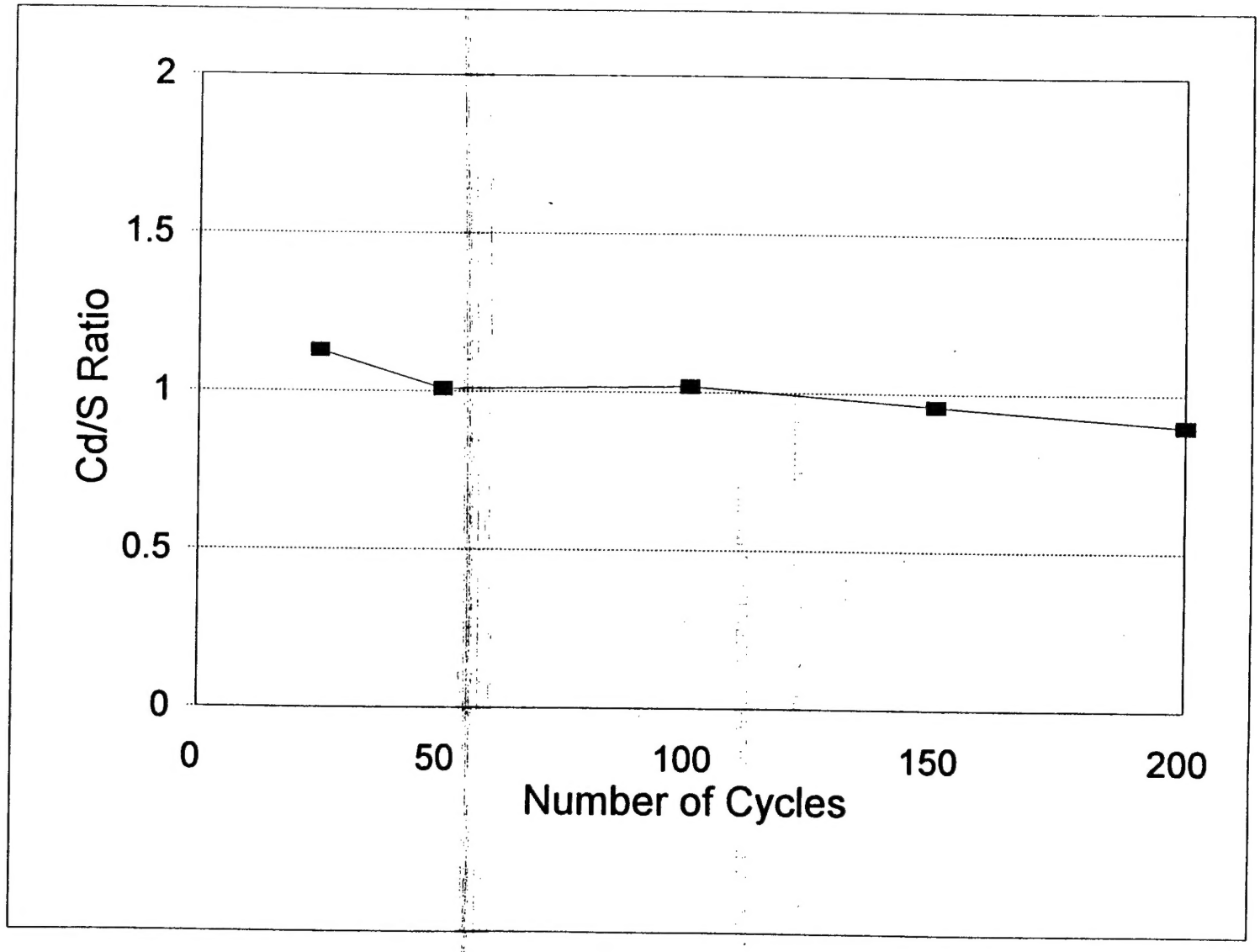
2
1.5
1
0.5
0
Cd/S Ratio
0
50
100
150
200
Number of Cycles